



Economic and design optimisation of a 15MW floating offshore wind platform using time-series forecasting

Craig White^{1,3}, Victor Benifla², José Cândido¹

- ¹ WavEC Offshore Renewables, Lisbon, 1350-352, Portugal
- ² University of Rostock, 18051, Rostock, Germany
- ³ Instituto Superior Técnico (IST), Lisbon, 1049-001 Portugal

Correspondence to: Craig White(craig.white@wavec.org)

Abstract. This work proposes a structural and economic optimisation framework applicable to floating semi-submersible platforms, demonstrated here for a 15-MW offshore wind design. A genetic algorithm was developed that can seek a multi-objective solution to minimise mass whilst respecting the constraints of loads acting upon the system. Statistical and machine learning methods are then employed to forecast near and far term costs of the platform under a range of scenarios. Finally, Levelized Cost of Energy is calculated to gauge the technical and economic viability. Results show that a mass reduction of 9% is possible. With optimal costs predicted under the SARIMAX scenario of 4404.56€/t, 24.1% under the average. The optimised platform results in an LCoE reduction of 2.08%.

15 1 Introduction

The deployment of floating wind turbines (FOWTs) into deeper waters offers access to stronger better wind resources, with less marine competition and lower visual impacts. Floating technology has witnessed rapid growth since the first full-scale prototype in 2009 (Skaare, et al., 2015), with pre-commercial status achieved in 2017 (Jacobsen & Godvik, 2021), 50MW in 2021 (Risch, et al., 2023) and 88MW in 2023 (Musial, et al., 2023). Costs have increased in the recent macroeconomic context and must decrease to achieve commercial deployment in the hundreds of megawatts (MW) and global installed capacity in the hundreds of gigawatts (GW) (DNV, 2023). Key areas of cost-reduction potential should be targeted first whilst maintaining strong reliability, offshore energy production and high farm availability to ensure competitive levelized cost of energy (LCoE) which will boost the chance of greater deployment. Floating offshore wind (FOW) must see LCoE reductions to become economically viable and compete with offshore wind and other renewable energy technologies, with the floating platform being a potential cost-saving area due to its large mass and typically steel construction (Barter, et al., 2020). This cost problem offers space for innovative solutions across three main areas: the dimensions of the platform itself, the materials used and their cost, and matching the design and dimensions to site conditions.

Market prices for key raw materials, including steel, have witnessed high volatility in recent years. Methods to accurately predict future prices would reduce risk and improve strategic planning for developers to minimise LCoE, especially for forecasts accurate within the lifetime of a project from initial feasibility to final investment decision (FID). Among these,

Preprint. Discussion started: 15 October 2025

© Author(s) 2025. CC BY 4.0 License.



40

45

50

55

60



time-series forecasting (TSF) methods using statistical and machine-learning models offer promising solutions by looking back at past trends to predict future values, to reduce risk and increase strategic long-term planning for floating offshore wind.

Currently, floating offshore wind does not have an integrated system design from nacelle to anchor, and relies on conventional offshore wind turbines attached to floating platforms. There are currently four main designs of platform that are yet to coalesce into an optimised standard. Barge-type allows for concrete and steel construction which lowers cost and can include a central pool to dampen wave action and floater motion. Tension-leg platform (TLP) design offers low mass and draft due to the tension stabilisation of the mooring lines, which transfers more loads to the mooring and anchoring system. Spar type designs are ballast-stabilised and have a simplified cylindrical design and higher draft. Semi-submersible designs are buoyancy-stabilised due to a wider platform, and therefore can operate in shallower waters. This concept has high mass and steel composition to achieve buoyancy stabilisation and can offer the opportunity for design minimisation through geometrical and thickness adjustments to the structural steel components: namely the inner column, outer columns, pontoons and upper supports.

Reference turbines and platforms offer valuable standardised designs that serve as a foundation for research and technology progression and provide a conservative layout, with a minimised chance of failure akin to prototype projects to ensure maximum offshore reliability. Due to its generic nature, the reference platforms serve as a basis for design improvements through geometrical adjustments to both the full system and sub-system components such as the columns and pontoons. This is the purpose of this paper: to optimise both the geometry and structural thickness of subsystems and the overall platform whilst ensuring that each design iteration adheres to acceptable levels of full-system load response based on the environmental design conditions that reflect a range of realistic offshore scenario probabilities. The IEA reference 15MW wind turbine (Gaertner, et al., 2020) is used alongside its partner UMaine reference Volturn-US-S (V-US) platform (Allen, et al., 2020) for this study.

2 Literature review

2.1 Support structure design

The engineering challenges for FOW including nacelle motion, wave sensitivity and the mooring system footprint are outlined (Butterfield, et al., 2005) and point towards how these have been overcome in the oil and gas (O&G) industry. A classification method is also presented for the variety of platform configurations into ballast, buoyancy and tension stabilization, noting that in practice designs are hybrid in nature, and an optimal point may be identified between all three, with serial production in high volume with onshore assembly offering economic benefit. If total platform cost reductions are within 25% then a competitive 0.05\$/kWh could be reached.

Conceptual and deployed semi-submersible foundations, as well as numerical simulation tools were reviewed in (Liu, et al., 2016). The same three classification methods based on stabilization were used, as these are the three main platform types

Preprint. Discussion started: 15 October 2025

© Author(s) 2025. CC BY 4.0 License.



65

70

90



expected for use in future scenarios. For semi-submersible platforms, three-legged, ring-shaped and V-shaped platforms, and the main numerical codes to investigate platform response to induced loads, were discussed. Due to the complexity of full-scale testing at sea, numerical modelling and tank-testing are preferable for the research of dynamic response, with springs used to represent the catenary mooring system in scale testing.

The IEA 15MW reference wind turbine (Gaertner, et al., 2020) forms the design basis for this study and for the V-US floating platform. The turbine was produced with a view to future upscaling trends in offshore wind where size constraints are not as strict as onshore. The 15MW was seen as a natural follow-on from the DTU 10MW (Bak, et al., 2013) and 5MW NREL (Jonkman, et al., 2009) and encompasses a three-bladed rotor, Class IB direct-drive generator, variable-speed and collective pitch controller, a rotor diameter of 240m and a hub height of 150m. The turbine is designed for a monopile foundation but has considerations and applicability for floating studies and follows the trend of offshore wind turbines for additional use for FOW. The VUS floater (Allen, et al., 2020) was designed to be paired with the 15MW turbine previously discussed to keep pace with the current offshore wind trend of ever larger wind turbines. The platform is of steel construction with three outer columns and pontoons connecting to a narrower central column that connects to the wind turbine tower interface. All significant geometric values and global coordinates link the design to aerodynamic, structural, and hydrodynamic numerical models such as OpenFAST and RAFT that is used in this study.

2.2 Numerical models

To accurately model the response behaviour of a floating turbine to offshore loads, all of the structural, aerodynamic and hydrodynamic effects should be considered. The coupled Dynamic Modelling of Floating Wind Turbine Systems (Wayman, et al., 2006) investigated the methods to achieve this joining the structural and aerodynamics of FAST with the numerical code of WAMIT for FOW systems in depths ranging from 10-200m. Coupled loads include the gyroscopic motion of the rotor on the tower and floating platform, and forces from wave excitation. Modelled motions were acceptable resulting from inputs including water depth and wind speed. An economic analysis was also conducted alongside a component-level costing which put the platform, moorings, and turbine install as key cost considerations. Final costs for the barge and TLP platform ranged from \$1.4-\$1.8 million respectively for a platform and mooring system, including installation for a 5MW system which shows the large range in platform costs.

The FAST model developed by the National Renewable Energy Laboratory (NREL) models the coupled response of floating wind turbines under realistic ocean conditions and was validated with the Statoil-Hywind 2.3MW demo floating wind turbine (Driscolla, et al., 2016). Site metocean measurements formed the model input conditions and the overall response of the platform and loads acting on it were in good agreement with measured data and validated the model's performance under these conditions and for the Hywind spar-type foundation.

A frequency-domain model for FOW design optimisation (RAFT) looks to the full integrated system, rather than just the platform combined with time-domain turbine processing (Hall, et al., 2022). Here, co-design of the support structure,

Preprint. Discussion started: 15 October 2025

© Author(s) 2025. CC BY 4.0 License.



95

100

110

115

120



turbine and controller are modelled in the frequency domain for added computational efficiency and design improvements. Three reference FOW designs were modelled and were compared with time-domain OpenFAST simulations. The dynamic response spectra and statistics performed well and within expected range that verified the model's application to FOW studies.

A review of modelling techniques for floating offshore wind turbines (Otter, et al., 2021) reiterated the challenges of the strong coupling of the turbine aerodynamics and the platform hydrodynamics, plus the Froude and Reynolds number scaling mismatch due to working with water and air fluid domains. It highlights the move towards high-fidelity modelling due to the cost and complexity of testing at scale, although not necessarily with CFD due to the long simulation times. The paper concludes that numerical modelling is a trade-off between accuracy and computational efficiency and that many numerical models require improvement, with CFD an option towards the end of the design phase. Physical testing can validate and calibrate numerical models and can be classed into full physical and hybrid testing, with the choice often down to facilities, budget, and test uncertainties.

105 **2.3 Floater response**

The influence of wakes and atmospheric stability on floater response by (Jacobsen & Godvik, 2021) studied the Hywind Scotland farm, in particular the wake interaction between turbines. Measurements of half of the six degrees of freedom that influence turbine motion (roll, pitch, yaw) were investigated and the wake effect of upstream turbines was found in the downstream devices. Atmospheric stability must be considered for offshore performance due to almost no wake effect observed under neutral and unstable conditions, but floater motions were found to be small at all studied wind speeds which credits the spar-shape design.

A 3D finite element analysis model for FOW support structures (Campos, et al., 2017) argued that common tools ignore the structural stiffness of the elements constituting the floating platform and are normally treated as rigid body. Flexibility was found to be crucial in structural lifetime analysis and this paper proposes a model to integrate the deformation of the structure within a fully coupled hydro-aero-servo-elastic time domain model. Hydrodynamic and aerodynamic loads are computed alongside the dynamic interactions between the turbine, structure, and internal forces. Results show good agreement between the model and experimental results, with maximum inclinations under 5° and nacelle accelerations 0.2g.

2.4 Design optimisation

A reliability-based design optimisation of a spar-type FOW support structure (Mareike & Kolios, 2021) is highly relevant when coupling economic efficiency with design uncertainties, especially when classification and standardization are not available. This is more complex with floating turbines and this paper presented a framework to address this. Environmental conditions, limits and uncertainties were specified and a reliability assessment approach defined which generated a response surface for various system geometries in the design optimisation. Using the example of a spar-type design, the method met all constraints including the reliability criteria and reduced platform and ballast mass.

https://doi.org/10.5194/wes-2025-197 Preprint. Discussion started: 15 October 2025

© Author(s) 2025. CC BY 4.0 License.



125

130

135

140

150

155



A software framework for a 22 MW Semisubmersible FOW platform (Zalkind & Bortolotti, 2024) was developed for the reference wind turbine of the same capacity. Different fidelity levels and the effect of varying load cases were evaluated for controller adjustment, plus the difference between sequential and simultaneous co-design. An algorithm that searches the design space before optimisation is suggested, and that solving smaller problems sequentially is advantageous rather than large simultaneous co-design solutions. Notwithstanding a more robust and reliable outcome, the simultaneous solution was found to produce a platform with 2% lower mass and therefore a trade-off between advantageous results and reliability is required.

An efficient optimisation tool for floating offshore wind support structures (Faraggiana, et al., 2022) highlights the need for economic competitiveness through a reduction of the platform weight and therefore structural cost. An optimisation tool applicable to any floating turbine is proposed that adjusts the geometry, in this case the OC3 spar-type design. The stability and dynamic performance was evaluated and optimised using a genetic algorithm (GA) coupled with a surrogate model to both minimise cost and maximise performance. Cost reductions across the best and worst cases of 2-3 times were found, with a 25% cost decrease between most and least restrictive optimal cases. Hydrostatic constraints were found to be more significant than dynamic ones due to influencing the design area.

As an optimal platform can be seen as a trade-off between weight and reliability, a multi-objective optimisation was developed (Qiua, et al., 2008) for three semi-submersible platforms using particle swam optimisation algorithm based on a surrogate model. Hydrodynamic performance was calculated using Morison's equation and the panel method, and the surrogate model was used to improve computational efficiency, with accuracy maintained using cross-validation. Platform weight and heave motion was selected as optimisation objectives, with metacentric height, surge motion and airgap as constraints. A multi-objective particle swarm method searched for optimal pareto fronts and was validated with a CFD tool. Heave motions could be reduced by 12.68-14.96% and total weight by 12.16-24.91%.

145 2.5 Genetic algorithm

A global optimisation tool identified and evaluated the configuration of support structures for FOW (Hall & Buckham, 2012). The rationale highlighted the nascent stage of FOW optimisation and the complex nature of FOW system interactions in multiple mediums that inhibit the convergence of designs. Also, geometrical optimisation has previously omitted key design parameters which drives the need for a flexible GA approach. Results show designs similar in nature to established spar and semi-submersible configurations, with others less conventional.

A GA framework was developed (Hall, 2013) to optimize the support structure for FOW using a nine-variable parameterization. This broadened the design space further than the state of art that considered a frequency-domain dynamics model linearized forces that recreated the physical considerations well acting on the turbine and support structure whilst remaining computationally efficient. The choice of GA allowed a visualisation of the design space and pareto front that showed optimal design choices, through minimization of both the support structure cost and root-mean-squared (RMSE) nacelle acceleration. Under \$6 million, three outer cylinders is optimal, with six cylinders when costs rise above \$6 million and heave

Preprint. Discussion started: 15 October 2025

© Author(s) 2025. CC BY 4.0 License.



160

165

170

175

180

185



plate size increasing with platform cost. The optimal complexity and unusual configuration of designs highlight improvements to the cost model.

In the literature, evolutionary algorithms, particularly GAs, are widely used for FOWT substructure design optimisation. These algorithms, inspired by biological evolution, operate with a population of individuals, each representing a potential design solution, which evolve through the design space. Genetic algorithms typically involve three main steps: selection, where individuals are chosen for the next generation or to produce offspring; crossover, where two parents are combined to create new individuals; and mutation, where random changes are introduced to maintain diversity. Each iteration, the fitness of the population is evaluated based on objective and constraint values, allowing the individuals to be ranked. While most follow this general procedure, there is significant flexibility in how these steps are implemented, leading to a variety of genetic operators and evolutionary strategies, which are well summarized in (Martins, 2022). GAs are extensively reviewed in (Sourabh Katoch, 2021), where different genetic operations and techniques are analysed. GAs are effective for both constrained and unconstrained optimisation problems, particularly when derivatives of the objective and constraint functions are complex to obtain. They are also well-suited for so-called "black-box" optimisation problems, where the function to be optimized is obtain through complex numerical models requiring time-consuming simulations. This makes GAs ideal for optimizing complex systems, such as floating offshore wind turbine substructure designs, where optimisation involves different design variables, complex numerical models and non-linear constraints.

2.6 Upscaling

The generic upscaling methodology to transfer a FOW turbine geometry from 5MW-15+MW was proposed (Wu & Kim, 2021), analysing the effects of changing the column radius and floating base. Results showed that upscaling the column radius increased the overall mass and natural heave period, whilst upscaling the column distance raised the centre of gravity and metacentric height of the system, with a slight lowering of the natural heave period that is important for semi-submersible designs. These issues can be minimized through added ballast mass to lower the centre of gravity and increased added mass to raise the natural heave period. A method of estimating the scaling of platform parameters was also provided for a range of turbine sizes and components.

A review of scaling laws applied to floating offshore wind turbines from 5MW-15MW (Sergiienko, et al., 2022) reiterates the upward trend in wind turbines and the need for platforms to also increase to support them. How the design and dynamics change with scale is investigated, with results showing that mass, rated power and rotor thrust scale close to the square of the rotor diameter, making it a useful consistent metric for parameter scaling with added rotor size. The paper also highlights that towers for FOW are usually thicker and heavier avoiding the wave excitation region matching the natural frequency. Regarding the platform geometry, there was a strong correlation found between the rotor diameter and the product of the offset columns and their diameter. Finally, design methods used by developers follow the square-cube scaling law when sizing platforms for larger wind turbines.

https://doi.org/10.5194/wes-2025-197 Preprint. Discussion started: 15 October 2025

© Author(s) 2025. CC BY 4.0 License.



200

205

210

215

220



2.7 Costs and LCoE

190 Feasibility of Floating Platform Systems for Wind Turbines (Musial, et al., 2004) shows a technical description of several floating platforms classed by mooring system method, especially the contrast between catenary and vertical systems. A cost comparison is provided between a semi-submersible tri-floater and a TLP developed at NREL, both supporting a 5MW turbine. Production costs are estimated at \$7.1 million for the semi-submersible and \$6.5 million for the NREL TLP. This reduces to \$4.26 million and \$2.88 million respectively under structural optimisation, bringing the cost of energy to the US Department of Energy target of \$0.05/kWh that the US Department of Energy necessary for large scale commercial FOW development.

Lifecycle LCoE (Myhr, et al., 2014) provided a detailed cost assessment of multiple support structures including spar, semi-submersible, and TLP. Mass-based calculations for platform cost were derived alongside the cost of mooring and anchoring systems, with depth and distance to shore found to be a dominant factor in LCoE. A large LCoE range of €82.0-€236.7 across substructures demonstrates the high variability and economic performance of designs. Further work recommended progression of cost calculations to include scaling effects for mass-produced components that is required for commercialisation of FOW, and tailoring components and overall system design to site conditions.

A systems engineering vision for FOW optimisation (Barter, et al., 2020) identified gaps to reduce the cost of energy, mainly through a full system-integrated approach to capture the complex interactions and physics across the lifecycle of a floating wind farm. A range of cost-reduction research areas are outlined including new substructures, anchoring methods, two-bladed and/or downwind rotors, alternative materials and FOW-specific controls. The paper argues that current engineering tools are inadequate to design systems that have cost-parity with the mature offshore wind sector. Flexible substructures, optimized turbine features and a geometry adaptive to the offshore environment are expected to be required. A multidisciplinary and multi-fidelity modelling approach that quantifies uncertainties is needed to achieve an optimal FOW system.

High potential cost-reduction areas should be targeted first to drive cost reductions in FOW. These can be split into 'soft costs' such as financing and project management and 'hard costs' that mainly relate to physical components that comprise the floating offshore turbine. These cost-reductions are realised through a combination of economy of scale (EoS) effects, learning rates achieved through increased cumulative deployment and design optimisation through research. Areas of high potential for floating offshore wind (FOW) were defined by (James & Ros, 2015) with a percentage reduction in costs from prototype to commercial scale. Installation is set for a 5% reduction, the balance of system (BoS) is expected to reduce by 9%, the turbine by 12% and the floating platform highest with a 16% reduction in CAPEX from prototype to commercial scale.

This work implements both accurate TSF models alongside structural optimisation to achieve a cost-minimised platform design across both the design space and the time domain, by predicting commodity prices for key floating platform components for strategic planning over the next fifteen years. A structural optimisation will first create multiple layouts within the design space and defined boundary constraints. The chosen optimised layout that minimizes the platform mass will then have expected aerodynamic and hydrodynamic loads applied using RAFT (Hall, et al., 2022) to the structure to confirm its

https://doi.org/10.5194/wes-2025-197 Preprint. Discussion started: 15 October 2025 © Author(s) 2025. CC BY 4.0 License.





suitability for a given range of sites and conditions. The cheapest layout that withstands acceptable loads will then pass to the economic optimisation phase: The best point of material purchasing will be obtained using the TSF model, to achieve an optimized system in the space, frequency, and time domains.

225 3 Method

230

235

240

245

250

This work can be divided into two main areas. First the platform mass minimization that is a combination of RAFT and a GA, which delivers a minimized mass that satisfies the overall constraints of the simulation. Second, the economic assessment that costs the floater based on short to medium-term forecasts of structural marine steel. Generalised project costs and power generation are then used to calculate the final LCoE over a range of future years to help strategize future floating offshore wind procurement.

3.1 Platform design

The main objective in this first part is to perform the design optimisation of a 15-MW semi-submersible platform. To do so, the design optimisation framework presented in (Benifla & Adam, 2023) is used and applied to the VUS substructure mounted with the IEA 15-MW reference offshore wind turbine (Gaertner, et al., 2020). In this study, the Response amplitudes of floating turbines (RAFT) open-source code is used to model the FOWT system in the frequency-domain and evaluate its static properties and dynamic response. The code has been validated against higher-fidelity tools such as OpenFAST and has shown good agreement while also being computationally efficient. This makes it an ideal choice for quickly evaluating various substructure designs under different environmental conditions (Hall, 2022).

In RAFT, the FOWT system is modelled as a rigid body with the common six degrees of freedom: surge, sway, heave, roll, pitch, and yaw. The dynamics are represented in the frequency domain, allowing the FOWT system to respond linearly to each excitation frequency. The complex amplitude of the system's response, X, at a given frequency ω , is obtained by solving the generic equation of motion for the FOWT system:

$$(-\omega^2 M + i\omega B + K)X(\omega) = F_{ext}(\omega), \tag{1}$$

where, M, B, and K represent the FOWT system's total mass, damping, and stiffness matrices, respectively, F_{ext} the external excitation forces, and ω the frequency. The frequency-domain dynamics of the FOWT are assumed to operate around a specific position, \overline{X} , which represents the mean steady state of the system. This position is obtained by solving iteratively the static equilibrium equation derived from the previous equation.

$$K_h = \overline{F}_{ext} + \overline{F}_{moor}(\overline{X}), \tag{2}$$



255

260

265

270



where \overline{F}_{ext} represents the mean external forces applied to the system, \overline{F}_{moor} is the nonlinear reaction force of the mooring system (accounting for the effective mooring stiffness), and K_h is the total hydrostatic stiffness.

In RAFT, the system can be evaluated under given environmental conditions defined by steady winds and stochastic sea states, characterized by a mean wind speed Ws and a JONSWAP wave spectrum with significant wave height Hs and peak period Tp. The rotor-nacelle assembly is modelled as a rigid body and with three identical blades with specific dimensions (chord, twist angle, and prebend) and distributed aerodynamic properties (lift and drag coefficients). The tower is defined as a cylindrical member, and the floating substructure as a combination of interconnected members of different shapes, with mass, inertia, buoyancy, and hydrostatic stiffness obtained by summing individual contributions. Mean aerodynamic loads are computed using a steady-state blade-element momentum solver, while mooring forces are determined with a quasi-static solver. The system's frequency response is obtained by linearizing the dynamic equations, accounting for rotor aerodynamics and hydrodynamic damping based on Morison's equation applied to discretized substructure strips. Finaly, RAFT computes the FOWT's mean offset and frequency-domain response, with maximum values estimated by combining the mean values and the complex response spectra. The maximum platform offset and other key quantities of interest—such as the tower-top nacelle acceleration and the tower-base bending moment in the fore-aft can be obtained. Different design load cases can be defined to include multiple wind and wave conditions, enabling a comprehensive evaluation of the system's dynamic response under various environmental scenarios.



Figure 1 – a) RAFT model of the V-US and the IEA 15MW in its static position (black) and maximum offset (red) when exposed to environmental conditions. b) Original design of V-US and c) Optimised design in red

A static stress analysis is performed to assess the structural integrity of potential designs. In this analysis the focus is at the vulnerable interface between the central column and pontoon. To estimate the loads, a free-body approach is followed, where the contributions of both the outer column and the pontoon itself are considered. Only considered here are structure weight and the buoyancy loads inducing moments on the structure interface. The stress on the pontoon base is:

https://doi.org/10.5194/wes-2025-197 Preprint. Discussion started: 15 October 2025 © Author(s) 2025. CC BY 4.0 License.





$$\sigma = M \frac{h_{po}}{2 \cdot I_{po}},\tag{3}$$

where M is the total bending moment, and h_{po} and I_{po} are the height and second moment of area of the pontoon section.

3.2 Design Optimisation

The main objective is to reduce the steel mass of the V-US platform under several constraints to account for the dynamic of the system. For a given design solution, represented by x, the constrained single-objective optimisation problem can be:

Minimize:

285 m(x)

295

300

305

Subject to:

$$\begin{aligned} X_{Li} &\leq X_i \leq X_{Ui} & i = 1, \dots, n_x \\ g_j(X) &\leq g_{jlim} & j = 1, \dots, n_g \end{aligned} \tag{4}$$

where m is the steel mass, X_{Li} and X_{Ui} denote the lower and upper limits of the design space and g_j is an inequality constraint with its associated limit g_{jlim} . These constraints are typically the output of the numerical analysis previously described that are monitored and constrained.

To solve, an efficient GA is implemented and inspired by (Hall, 2013). This was applied to FOWT substructure design, and addresses limitations of traditional evolutionary algorithms by identifying local optima and avoiding unnecessary problem evaluations. A distance-weighted scaling operation is performed to ensure that each local optimum identified within the population are treated equally. Throughout the optimisation, the fitness of the entire population is scaled, leading to the total scaled population fitness as described in (Hall, 2012). This is combined with a constraint-handling technique used by (Deb, 2000) allowing infeasible solutions to be compared solely based on their total constraint violation. This form of the penalty enables a clear comparison between feasible and infeasible solutions, allowing the GA to handle constraints effectively.

The initial population is generated and evolves by using Simulated Binary Crossover (SBX) and a polynomial mutation operation, originally introduced in (Deb, 1995). These efficient operators are widely used addressing real-valued optimisation problems. After new offspring are generated, they are assessed before being added to the current population. This ensures that they not too alike existing individuals while remaining close to fit ones. The check avoids the computational cost of evaluating the problem for individuals not added. This approach is particularly beneficial here, as evaluating the objective and constraint functions requires significant computational resources to run the numerical models described. It also ensures that the population evolves toward fitter regions of the design space, resulting in lower population density in less fit areas. The structure of the framework is shown in Figure 2 and illustrates the interaction between the GA and the RAFT dynamic model.





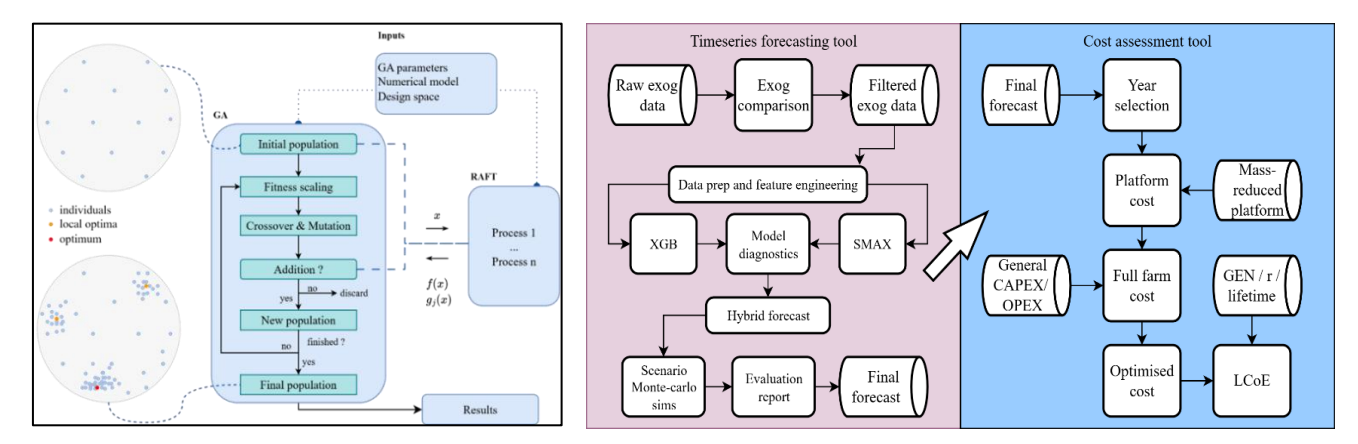


Figure 2 - Process flow of a) Design optimisation and b) Timeseries forecasting and cost assessment tool

3.3 Price forecasting and economic assessment

After the design optimisation of the platform, an economic assessment is applied to the mass-minimised and constraint-respected structure that encompasses cost predictions using time series forecasting and an economic platform assessment. First, a range of future costs up to seven years ahead are calculated using a combination of timeseries forecasting methods. Second, these costs are applied to the mass-minimised structure to derive a cost at platform and farm level, plus subsequent LCoE.

3.3.1 Price forecasting

The price forecasting tool is a combination of a short-term machine learning XGBoost (XGB) model and a statistical SARIMAX (SMAX) model for the medium to long-term. The output forecast is blended to capture stochastics and long/term trends to achieve a minimisation of MAE, RMSE, and model metrics (BIC, AIC). Both short and medium-term models rely on exogenous data (exogs) that are provided in the form of monthly prices, indices and other economic metrics that support steel price forecasts. The equation for XGB can be found:

$$L\phi = \sum_{i=1}^{n} I(y_i, \hat{y}_i) + \sum_{k=1}^{K} \Omega(f_k),$$
 (5)

Where $L\Phi$ is the total objective function, $I(y_i, \hat{y}_i)$ the loss function between measured and predicted values, $\Omega(f_k)$ the regularization term which marks down complexity to reduce overfitting, f_k the k-th weakest decision tree learner in the group, and k the total number of decision trees. For SARIMAX:

$$y_t = \mu + \phi(B)\Phi(B^S)(1 - B)^D y_t + \theta(B)\Theta(B^S)\varepsilon_t + \beta X_t, \tag{6}$$

330

315

320

https://doi.org/10.5194/wes-2025-197 Preprint. Discussion started: 15 October 2025 © Author(s) 2025. CC BY 4.0 License.



335

340

345



These are data of equal length and granularity to the predictor, such as raw material prices, metal indexes and economic indicators including imports, exports and gross domestic product, both domestic and international. The exogs are processed, cleaned and filtered from raw data using statistical comparison metrics including p/r value on a change log scale. A sheet is created for the forecaster model that contains the best exogs from the comparison to aid predictions. Data is then cleaned and aligned to create training and testing splits, with most datasets ranging from 2009-2025, with the full process seen in Figure 2.

The short-term machine learning XGBoost (XGB) model is used for the initial forecast, usually set to 12-36 months and selected due to an ability to understand stochastic short-term patterns in the data, as well as the acceptance of exog data akin to the SMAX model. Data protections are included so that the model is trained per horizon, and that it cannot cheat and see future data in the test section, as this is easy to do and results in "too good to be true" forecasts. Both models are evaluated based on a rolling cumulative validation, judged using mean average error (MAE), root mean squared error (RMSE) and model evaluation criteria: Akaike and Bayesian Information Criteria (AIC/BIC). The medium to long-term SMAX from the start of the forecast window but over a longer period, up to a maximum seven years. An optimisation loop finds the model parameters which deliver the lowest evaluation criteria akin to the XGB forecast. A hybrid forecast then combines the two, selecting automatically the best fitting model for each section, which generally is XGB for the first 12-24 months and then blended into SMAX which creates the forecast used to cost the semi-submersible platform. A final evaluation tests the forecasts against past windows with guards against data leakage, with added evaluation metrics to check the performance of the hybrid forecast.

3.3.2 Economic assessment

With a hybrid forecast defined for up to seven years, platform costs from literature (BVG, 2025) transform the HRC steel prices into platform cost data. Only the primary steel mass is impacted by the price forecasts in this study, which forms almost the entire cost. Other platform components including secondary steel items, ballast and controls are costed from literature, as they are not the main subject of this study and primary steel contributes around 83% of the total platform (BVG, 2025). Other wind farm costs are generalised again from (BVG, 2025) to remove site-specific and project bias, with primary steel mass of the platform removed to allow space for the optimised platform. A net capacity factor of 0.4925 that considers all losses including electrical are used for a floating offshore 1GW wind farm (Beiter, 2020), validated with a gross CF of 0.5024 (Martini, 2016) to arrive at an LCoE value per year of the forecast. LCoE is then placed within the current framework of to see how both the economic and structural design optimisation influence both platform cost and LCoE.

4 Results

360

4.1 Platform design

The design of the V-US platform is composed of one centre and three outer columns linked through pontoons and upper supports. Here, the design variables are continuous real values and defined as the main platform diameter (D), the centre and outer columns diameters (d_{cc} , d_{oc}) and the height, width and thickness of the pontoon (h_{po} , w_{po} , t_{po}). This design

Preprint. Discussion started: 15 October 2025

© Author(s) 2025. CC BY 4.0 License.



365

370

375

380

385

390



parametrization is highlighted in Figure 3. Any other design parameters for the substructure, mooring system, or turbine remain fixed and their values are from the base model.

The objective of this design optimisation problem is to minimize the total mass while ensuring its dynamic performance. The FOWT system is evaluated in terms of dynamic responses under a reduced set of load cases. While the environmental conditions in this study are not site-specific, they were selected based on experience values and previous design optimisation studies (Dou, 2020) to represent typical conditions that need to be assessed for the development of FOWT substructures according to standards. Typically, these must include the rated wind speed of the rotor and harsh sea states to represent worst cases scenarios. Additionally, the three representative environmental conditions are chosen to reflect typical values for rated mean wind speed and sea state encountered in Europe, as seen in (Messmer, 2023). It is also worth noting that there is no wind-wave misalignment and that the mean wind force is normal to the rotor plane.

Table 1 - Design load conditions for design optimisation

	Wind sped	Sig. wave height	Sig. wave period
DLC	Ws (m.s-1)	Hs (m)	Tp(s)
1	9	6.3	11.5
2	11	8.3	12.95
3	25	9.9	14.1

In this design optimisation study, the dynamic performance of the FOWT system is evaluated with constraints on specific aspects of the platform response and turbine behaviour. The maximum platform offset, the platform pitch, and the nacelle acceleration at the top of the tower in the wind direction are constrained ensuring these values remain within acceptable limits. Finally, the fore-aft bending moment at the tower base and the static stress at the location at the interface between the central column and the pontoons are also considered and limited as they represent the stress that can be transferred to the substructure and is commonly limited in design. Each of these constraints values are computed for each defined load case and the maximum result across all cases is selected to be checked against the constraint limits of the optimisation problem. Defining these constraint limits to accurately represent real-world conditions can be challenging, so they are often set to general values based on experience. This approach is also applied here, supported by insights from previous optimisation and simulation studies and other publicly available models of the V-US.

The main inputs for the design optimisation study presented here are gathered and summarized in Table 1. Due to the inherent randomness of GAs the design optimisation problem is run 10 times to collect statistical results from multiple optimisation runs and properly assess the results and efficiency. For each run, the population starts at 100 individuals and the maximum number of generations is capped at 1000 for a reasonable amount of evaluation for this large design space. The following figure shows the steel mass evolution of the best individual in the population through its evolution for all the runs.





This shows the good behaviour of the algorithm that minimize the objective while reaching feasible regions of the design space where constraints are respected.

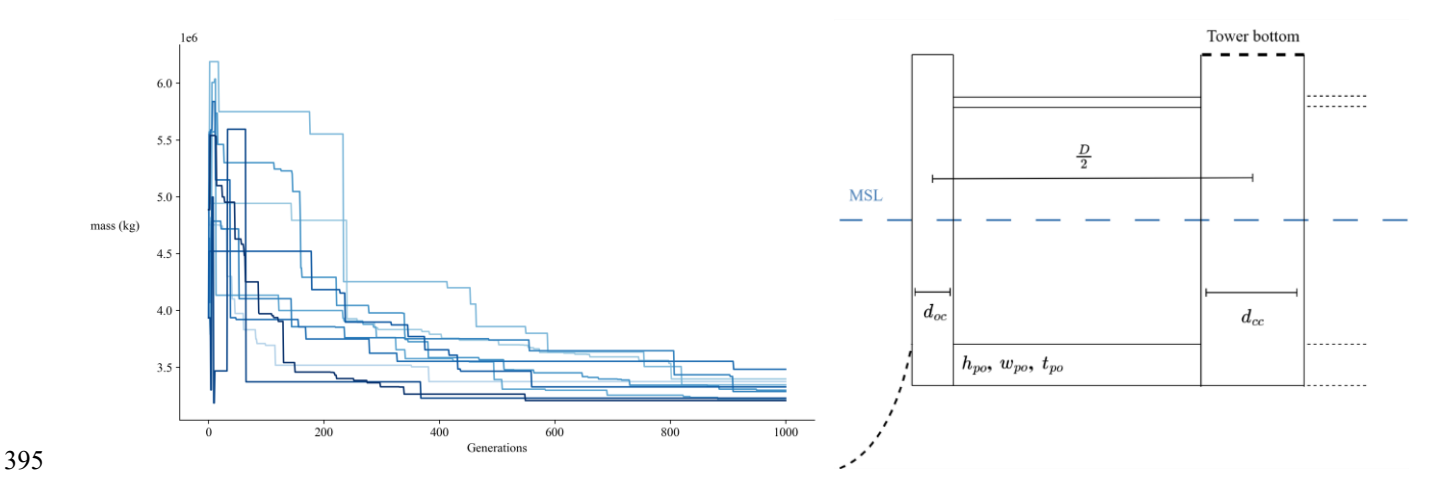


Figure 3 – a) Mass/objective evolution for multiple runs b) Cross section of substructure and design parameters

The statistical results collected from the 10 optimisation runs showed consistent performance, with small standard deviations and some small variation between the run outputs. These results also shows that the algorithm led to near optimal solutions in some runs highlighting the importance of repeated optimisation. Out of all the runs, the chosen optimized design is gathered and compared with the base model shown in Figure 1 (black base, optimised red) and the following Table 2. The worst successful design is chosen for the rest of this work so that it constitutes a safety margin that encapsulate some of the aspect neglected here. As expected, the mass is minimized while keeping the dynamic behaviour of the system as well as its structural integrity. The optimized mass obtained can be considered quite low when compared to the original, but this is anticipated as the structural check of potential designs is relatively simple here and lacks more in-depth analysis of the structure behaviour in terms of dynamic stress analysis. Mainly the optimized design exhibit slightly larger outer columns and pontoon dimensions but with a smaller platform diameter. Indeed, the design optimisation work presented here allows for a first optimized design that can be considered in the subsequent economic analysis. For further detailed analysis, once could consider other environmental analysis design space and enhance structural analysis to reach more confidence in the final optimize design.

Table 2 – Main characteristics of platform design and loads

	Symbol	Units	Bounds	Original	Optimized
Diameter	D	m	[50, 150]	103.5	100.46
Diameter (central col)	D_{cc}	m	[10, 30]	10	10
Diameter (outer col)	D_{oc}	m	[5, 30]	12.5	14.46
Pontoon width	w_{po}	m	[5, 15]	12.4	13.98

400

405



410

415

420



Pontoon height	h_{po}	m	[5, 15]	7	8.58
Pontoon thickness	t_{po}	m	[0.001, 0.1]	0.05	0.032
Mass		t	-	3916	3611
Offset (m)		m	[0,25]	23.13	22.7
Pitch (°)		0	[0,5]	5.7	4.83
Tower bending moment		MNm	[0,600]	496.89	553.11
Nacelle acceleration		m/s^2	[0,3]	1.76	2.12
Sigma		MPa	[0,300]	161.8	299,8

4.2 Time series forecasting

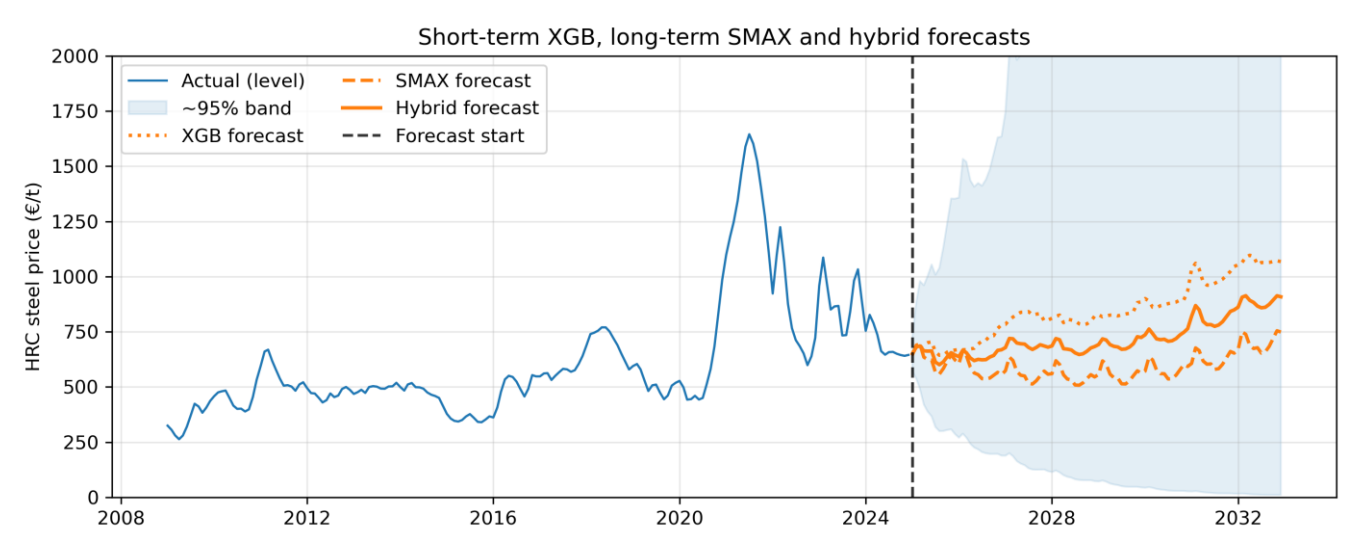


Figure 4 - Short to long-term forecasts of HRC steel prices using XGB, SMAX and hybrid forecasts

The actual, XGB, SMAX, and hybrid forecasts are shown in **Figure 4**, with actual HRC steel price data running from 2009-2025, and the forecasts from 2025-2032. Seven years was deemed suitable for forecasts due to the difficulty in obtaining long term forecasts, especially for volatile commodities. Also, most floating offshore wind procurement schedules at commercial-scale are expected to the be from four to seven years which was the ideal range for this study. The SMAX forecasts was trained using an 80/20 train/test split as was the XGB model. SAMX forecast is the most optimistic price-wise and also most sensitive to model changes which are inherent to achieving reliable forecasts, including seasonality, differencing, and others. With long computational times. The recent market volatility can be seen in the peaks within the data, decaying over time but with an overall dip in prices until 2030. For XGB, it is the most pessimistic of predictions, expecting higher prices that have small peaks and generally climb until the end of the forecast period in 2032. The hybrid is not necessarily the average of the two forecasts, and selects the best forecast on a rolling evaluation window. As the model does blend the forecasts, above with an overall 50-50 split, the hybrid is almost a mean value that serves as mid-point scenario in this study.



425

430

440

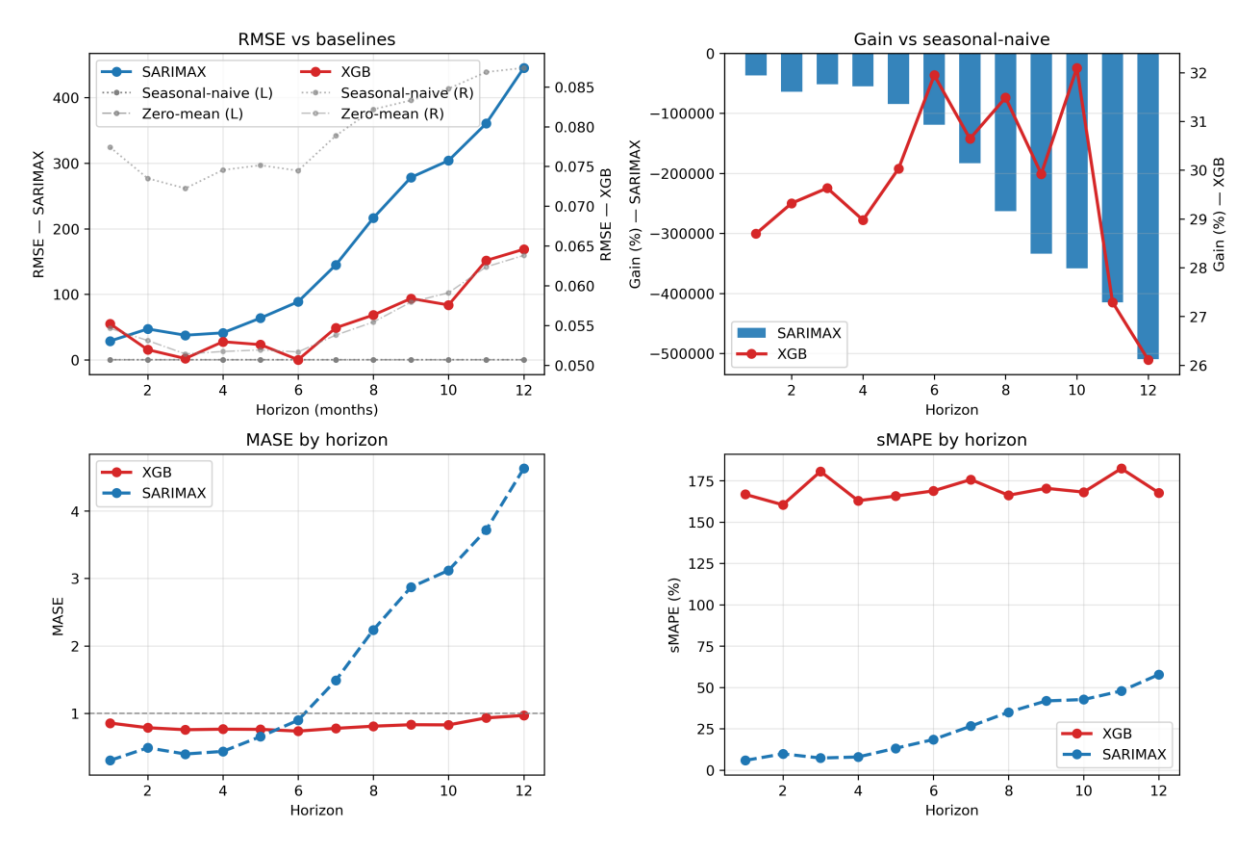


Figure 5 - Diagnostic analysis of XGB and SMAX forecasts against the seasonal-naïve forecast

An evaluation of the XGB and SMAX models can be seen in Figure 5, with good model performance against the seasonal naïve with lower root mean square error (RMSE), especially for the XGB and better performance. It is expected for RMSE to climb towards the end of a forecast period but this is more sudden for the SMAX model. The XGB model is more stable and at this stage a more reliable predictor, with the SMAX forecast performing better at shorter forecasts. Overall, the models perform better than the baseline repetitive forecasts which does not change over time, the SMAX model requires further tuning for long term forecasts or perhaps different exog data.

435 4.3 Economic assessment

The steel price and LCoE with changing forecast year are shown below in Figure 6, for the three scenarios and for the two types of platform: Initial (ini) mass of 3912t and Optimised (opti) 3481, which is the best and consistent outcome from the GA model. As the platform cost is applied across the forecast window consistently, results follow the trend of the three predictions with SMAX offering a minimised steel price (marine-grade) of under €4500/t in 2028, with LCoE at around 162-166€/MWh depending on platform optimisation. With the platform mass reduction resulting in LCoE savings of approximately 2.08%,





with the biggest gap occurring during the XGB forecast. All three scenarios do show an overall upwards trend in steel price in the medium to long term, with SMAX prices starting to climb from 2029 onwards.

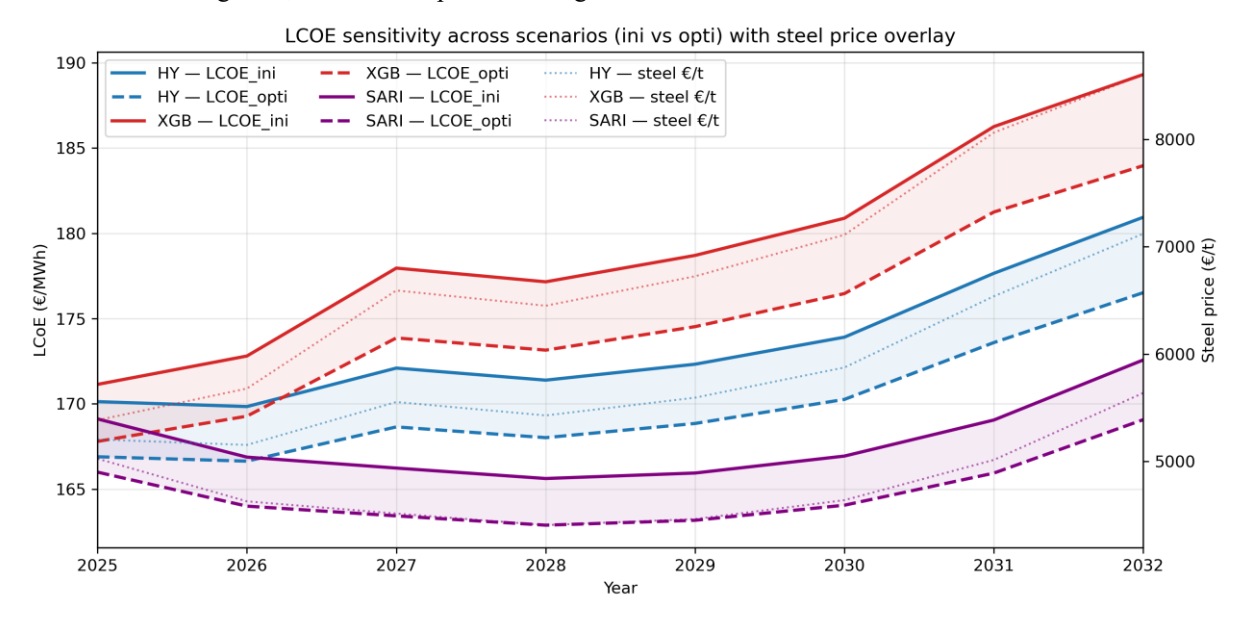


Figure 6 - Platform total cost and LCoE for platform and forecast type

445 5 Conclusions

450

455

This work presented the combination of a platform mass minimization whilst respecting design constraints, and an economic assessment that costed the platform now and into the future using a combination of forecasting methods. The LCoE was estimated using general costs and energy generation from wider literature, which placed the system within both a 1GW farm scale and within the current LCoE framework. Results show that design improvements are possible for the reference platform whilst still respecting the constraints of expected loads acting on the floating turbine in the offshore environment.

For cost forecasting, it is possible to blend forecasts to take advantage of the benefits of short-term models that can capture stochastic fluctuation, and also longer-term statistical models that can capture deeper trends in time-series data. In this research the XGB outperformed the SMAX model and more calibration is required to build confidence in future predictions. The models did however perform better than seasonal naïve forecasts which assume no change and give promise to the ability to predict future commodity prices that can help inform the procurement process and development of floating offshore wind.

References

Allen, C. et al., 2020. Definition of the UMaine VolturnUS-S Reference Platform Developed for the IEA Wind 15-Megawatt Offshore Reference Wind Turbine, Golden, CO: National Renewable Energy Laboratory.

Bak, C. et al., 2013. The DTU 10-MW reference wind turbine, s.l.: Danish wind power research.





- 460 Barter, G. E., Robertson, A. & Musial, W., 2020. A systems engineering vision for floating offshore wind cost *Renewable Energy Focus*, Volume 34.
 - Beiter, P. M. W. D. P. C. A. S. M. H. D. a. O. M., 2020. *The cost of floating offshore wind energy in California between 2019 and 2032*, Golden, CO (United States).: National Renewable Energy Lab (NREL).
- Benifla, V. & Adam, F., 2023. of Floating Offshore Wind Turbine Substructure Using Frequency Domain Modelling and Genetic Algorithm. Trondheim, s.n.
 - Butterfield, S., Musial, W. & Jonkman, J., 2005. Engineering Challenges for Floating Offshore Wind Turbines. Copenhagen, Denmark, s.n.
 - BVG, 2025. Guide to a Floating Offshore Wind Farm, s.l.: BVG.
 - Campos, A., Molins, C., Trubat, P. & Alcaron, D., 2017. A 3D FEM model for floating wind turbines support structures.
- 470 Trondheim, Norway, s.n.
 - DNV, 2023. Energy Transition Outlook, s.l.: s.n.
 - Driscolla, F. et al., 2016. Validation of a FAST Model of the Statoil-Hywind Demo Floating. Trondheim, Norway, s.n.
 - Faraggiana, E. et al., 2022. An efficient optimisation tool for floating offshore wind support structures. *Energy Reports*, Volume 8, pp. 9104 9118.
- 475 Gaertner, E. et al., 2020. *IEA Wind TCP Task 37: Definition of the IEA Wind 15-Megawatt Offshore Reference Wind Turbine (Technical Report)*, Golden, CO: National Renewable Energy Laboratory.

Hall, M.

- Hall, M. & Buckham, B., 2012. GENETIC ALGORITHM-BASED PLATFORM FOR FLOATING OFFSHORE WIND TURBINES. Vancouver, Canada, s.n.
- 480 Hall, M., Housner, S., Zalkind, D. & Bortolotti, P., 2022. *An Open-Source Frequency-Domain Model for Floating Wind Turbine Design* Delft, Netherlands, s.n.
 - Jacobsen, A. & Godvik, M., 2021. Influence of wakes and atmospheric stability on the floater responses of the Hywind Scotland wind turbines. *Wind Energy*, 24(2), pp. 149-161.
- Jacobsen, A. & Godvik, M., 2021. Influence of wakes and atmospheric stability on the floater responses of the Hywind Scotland wind turbines. *Wind Energy*, Volume 24, pp. 149-161.
 - James, R. & Ros, M. C., 2015. Floating offshore wind: market and technology review, s.l.: The Carbon trust.
 - Jonkman, J., Butterfield, S., Musial, W. & Scott, G., 2009. *Definition of a 5-MW Reference Wind Turbine for Offshore System Development.*" (2009)., s.l.: National Renewable Energy Laboratory (NREL).
- Liu, Y., Li, S., Yi, Q. & Chen, D., 2016. Developments in semi-submersible floating foundations supporting wind turbines: A comprehensive review. *Renewable and Sustainable Energy Reviews*, Volume 60, pp. 433-449.
 - Liu, Y. et al., 2018. Response Characteristics of the DeepCwind Floating Wind Turbine Moored by a Single-Point Mooring System. *Applied Sciences*, Volume 8.





- Mareike, L. & Kolios, A., 2021. of a spar-type floating offshore wind turbine support structure. *Reliability Engineering & System Safety*, Volume 213.
- 495 Martini, M. G. R. A. J. L. I. a. V. C., 2016. Met-ocean conditions influence on floating offshore wind farms power production. *Wind Energy*, 19(3), pp. 399-420.
 - Martins, J. R. R. A. a. N. A., 2022. Cambridge, : Cambridge University Press.
 - Musial, W., Butterfield, S. & Boone, A., 2004. Feasibility of Floating Platform Systems for Wind Turbines. Reno, Nevada, s.n.
- 500 Musial, W. et al., 2023. *Offshore wind market report: 2023 edition*, Golden, CO: National Renewable Energy Laboratory (NREL).
 - Myhr, A., Bjerkseter, C., Ågotnes, A. & Nygaard, T., 2014. Levelized cost of energy for offshore floating wind turbines in a life cycle perspective. *Renewable Energy*, Volume 66, pp. 714-728.
- Otter, A., Murphy, J., Pakrashi, V. & Robertson, A., 2021. A review of modelling techniques for floating offshore wind turbines. *Wind Energy*, Volume 25, pp. 831-857.
 - Qiua, W. et al., 2008. of semi-submersible platforms using particle swam *Ocean Engineering*, Volume 178, pp. 388-409.
 - Risch, D. et al., 2023. Characterisation of underwater operational noise of two types of floating offshore wind turbines, s.l.: Scottish Association for Marine Science (SAMS).
- Sergiienko, N. et al., 2022. Review of scaling laws applied to floating offshore wind turbines. *Renewable and Sustainable Energy Reviews*, Volume 162.
 - Skaare, B. et al., 2015. Analysis of measurements and simulations from the Hywind Demo floating wind turbine. *Wind Energy*, 18(6), pp. 1105-1122.
 - Sourabh Katoch, S. S. C. a. V. K., 2021. A review on genetic algorithm: past, present, and future. *Multimedia tools and applications*, 80(5), pp. 8091-8126.
- Wayman, E. et al., 2006. Coupled Dynamic Modeling of Floating Wind Turbine Systems. Houston, Texas, s.n.
 - Wu, j. & Kim, M.-H., 2021. Generic Upscaling Methodology of a Floating Offshore Wind Turbine. *Energies*, Volume 14. Zalkind, D. & Bortolotti, P., 2024. *Control Co-Design Studies for a 22 MW Semisubmersible Floating Wind Turbine Platform*. Firenze, s.n.